Hindawi
Advances in Materials Science and Engineering
Volume 2023, Article ID 7231516, 17 pages
https://doi.org/10.1155/2023/7231516

Research Article

Effect of Crumb Rubber on the Moisture and Rutting Behavior of Low-Energy Asphalt and Determining the Best Flow Number Model

Saeid Moghimi,[1] Gholamali Shafabakhsh ,[1] and Hassan Divandari [2]

[1]*Department of Highway and Transportation Engineering, Faculty of Civil Engineering, Semnan University, Semnan, Iran*
[2]*Department of Civil Engineering, Central Tehran Branch, Islamic Azad University, Tehran, Iran*

Correspondence should be addressed to Gholamali Shafabakhsh; ghshafabakhsh@semnan.ac.ir

Received 17 November 2022; Revised 7 May 2023; Accepted 13 June 2023; Published 22 June 2023

Academic Editor: Sharanabasava Ganachari

The advancement of technology and the increasing growth of environmental threats have led experts in the field of transportation to find alternatives for hot mix asphalts (HMAs). One of these alternatives is low-energy asphalt (LEA) mixtures. LEA mixture consists of hot asphalt binder and coarse aggregates and wet sand, which, having a lower mixing temperature, has caused a significant reduction in energy consumption and pollutants emitted from asphalt binder. According to previous studies, the influence of crumb rubber (CR) on the rutting and moisture performances of LEAs has not been investigated so far. In this regard, due to the softness of this type of asphalt mixture and its weakness against rutting and moisture, in this study, as an innovation, CR was used to modify LEA mixtures in three weight percentages of 10, 15, and 20. Considering the high moisture sensitivity of LEA mixtures due to the presence of water, the ability of CR to overcome this weakness and its potential to be replaced with antistriping additives were also investigated using the indirect tensile strength (ITS) test. In addition, in order to evaluate the rutting resistance, LEA mixtures were subjected to the dynamic creep test at a temperature of 54.4°C and at two stress levels of 270 and 310 kPa. According to ITS test results, it was found that although the modified LEA mixtures with 10 and 15% CR met the minimum requirement, the tensile strength ratio (TSR) value recorded for mentioned mixtures was still lower than that for HMA. Therefore, it is recommended to use antistripping additives in the use of LEA-containing CR, especially in areas with a high probability of moisture damage. The results of creep curves and flow numbers (FNs) extracted from four different models of three-stage, Fnest, Francken, and stepwise showed that although the LEA sample without additive had lower rutting resistance than HMA, the modification of this mixture to 15% CR significantly increased the rutting resistance. Moreover, considering the variety of variables in the process of making LEA compared to HMA, the comparison of FN determination models and the introduction of the most stable model were conducted in this research. According to the laboratory and statistical analysis results, it was found that the Francken model had less sensitivity to the variables, so it is suggested to determine FN for LEA mixtures.

1. Introduction

Today, with the advancement of technology, negative effects, such as environmental pollution, are the most important threat to human societies. The emission of greenhouse gases has resulted in global warming and climate change [1–3]. One of these polluting factors is the production of hot mix asphalt (HMA), which has a high consumption of fossil fuels and releases many pollutants due to the high production temperature (150–180°C). Increasing concerns about the preservation and protection of the environment led many researchers to find alternatives for HMAs [4, 5]. One of these efforts is to achieve warm mix asphalt (WMA), which has led to the production of asphalt mixture at a temperature of 110–140°C by using cleaner technologies [6]. Recently, with more attention to sustainability issues in the road pavement industry, there have been innovations to produce mixtures at a temperature of 60–100°C. This asphalt mixture is called half-warm mix asphalt, which has presented many environmental benefits with acceptable performance [7].

LEA mixtures are part of half-warm mix asphalts, which were produced at a range of 80 to 100°C by LEA-Co in France in 2006 [8]. This asphalt mixture is produced in such a way that after separating the aggregates into two sections, coarse and fine, first the coarse aggregates are heated to 170°C, and then, they are mixed with hot asphalt binder. After ensuring proper asphalt coating, fine aggregates are added at ambient temperature with desired humidity. The contact of moisture with a hot mixture produces foam, increases the asphalt binder volume, and results in a slow decrease in viscosity. Among the benefits of production, this asphalt mixture is a significant saving in energy consumption. Since fine aggregates are added wet to the mixture, there is no need to dry them, and therefore, fuel consumption is lower in the production process. Also, low production temperature results in less emission of greenhouse gases from asphalt binder. In addition, the reduction of asphalt binder viscosity due to the foam formation and its less aging due to the low production temperature causes the mixture to soften, and as a result, the mixture has better compactability. Greater safety during execution and less consumption of solvent to clean the equipment at the end of daily operations are other benefits of using LEA [9].

Despite the above advantages, since the moisture sensitivity of asphalt mixtures affects their performance, the investigation of moisture damage is a fundamental challenge in their use. Moisture damage occurs due to weak adhesion and lack of cohesion in asphalt mixtures. Half-warm asphalt mixtures and especially technologies based on asphalt binder foam have less adhesion between asphalt binder and aggregates [10]. Also, less asphalt binder coating on aggregates due to the low viscosity of asphalt binder causes lower integrity of these mixtures. Studies conducted on LEA mixtures show that moisture damage is one of the weaknesses of this asphalt mixture. In this regard, in the evaluation of moisture resistance by Zelelew et al., by determining indicators, such as Humburg stripping slope and Humburg inflection point, it was indicated that LEA mixtures have a lower moisture resistance than HMA mixtures [11]. Also, the results of the moisture resistance test in the research conducted by Olard et al. showed that the LEA sample has a lower moisture resistance than the HMA sample. In this evaluation, the r/R ratio (in which r is the compressive strength of samples stored in water and R is the compressive strength of samples stored in the air) in the Duriez test (NF P 98 251-4) was reported to be almost 10% smaller than the ratio obtained for HMA sample [12]. In addition, in the research carried out by Some et al., the evaluation of the moisture sensitivity of asphalt mixtures according to EN 12697-12 indicated a lower moisture resistance for LEA than HMA [13]. Therefore, due to the low moisture resistance of LEA and due to the presence of water in its production process, the use of an additive capable of increasing adhesion and reducing moisture sensitivity is emphasized to compensate for this deficiency.

Also, the other important weakness of half-warm asphalt mixtures, including LEA, is the high sensitivity of these asphalt mixtures against rutting. Due to the low mixing and compaction temperatures, the asphalt binder faces less aging, so this mixture is softer compared to HMA and has less rutting resistance [14]. Rutting or permanent deformation is the accumulation of permanent strains at the place of vehicle wheel loading, which leads to a decrease in pavement performance and service quality [15]. Despite extensive research on the rutting resistance of half-warm mix asphalt, little research has been performed on the susceptibility of LEA mixtures against this failure. Among the studies conducted in this regard, we can note a study presented in the NCHRP report 691, in which the dynamic creep test was used in order to evaluate the rutting resistance, and four asphalt samples including LEA, HMA, a sample modified with Advera, and a sample modified with Sasobit were tested. According to the findings, the highest value of flow number (FN) was assigned to the sample modified with Sasobit, and the lowest value of this parameter was recorded for the LEA sample. In this evaluation, the HMA sample showed much higher resistance to rutting by recording FN about twice the LEA sample. Also, the sample containing Advera was in a better condition than LEA with a slight difference in FN value. In the other part of this research, the rutting resistance of LEA was evaluated by conducting the dynamic modulus test and comparing it with HMA. The master curve drawn from the test results showed that LEA is significantly softer than HMA. In this research, by increasing one level in the high-temperature grade LEA sample, it showed better rutting resistance, so that the rutting depth for this mixture reached 0.05 inches with a significant reduction [16]. Zelelew et al. studied the rutting resistance of LEA by conducting a wheel track test using the Hamburg method. For this purpose, the number of wheel passes regarding 20 mm rut depth was evaluated. According to the results, HMA has the highest rutting depth followed by warm mix asphalt (WMA) samples containing Sasobit and Advera. In this evaluation, the sample containing Gencor and LEA sample, respectively, showed the weakest rutting resistance [11].

In the process of urbanization and construction [17, 18], a large number of waste materials are produced, one of which is waste tires in the field of automobile manufacturing [19]. Urban infrastructure is important to promote sustainable development [20–22]. These waste rubber materials are difficult to degrade naturally, and incineration and landfill will do some harm to the environment and also bring financial losses to societies. Crumb rubber (CR) is one of the most significant asphalt modifiers utilized in several years in the pavement industry, which is reclaimed from the tires of vehicles. CR application in asphalt mixtures has been examined for several years as a suitable additive for enhancing the properties of unmodified mixtures and crumb tire removals. Previous research showed that the use of CR as a thermoplastic elastomer in virgin binders enhances the characteristics of asphalt mixtures to rutting, moisture, and fatigue, decreases the maintenance and rehabilitation costs of mixtures, improves pavement life, and reduces traffic noises [23]. By mixing CR and asphalt binder, CR is immersed in the asphalt binder and quickly undergoes a physicochemical reaction. This two-stage reaction includes swelling and degradation, which is a function of mixing time

and temperature. At first, with increasing temperature, aromatic oils are absorbed by polymer chains of rubber and physically cause swelling of rubber particles. By increasing the size of the rubber particles and decreasing the oil part of the asphalt binder, the interparticle distance decreases. This causes the formation of a gel-like structure in the asphalt binder and increases its viscosity greatly. By increasing the temperature and mixing time, the swelling reaches the point where the rubber undergoes degradation. This part of the reaction has a chemical nature and includes devulcanization and depolymerization, which occurs by increasing the temperature up to 260°C after a few hours and a shear of 8000 rpm [24]. On the other hand, the studies conducted regarding the use of CR to modify asphalt binder show that the complete reaction of CR in asphalt binder has a negative effect on its characteristics. Also, raising the temperature leads to the destruction of asphalt binder networking. Therefore, the greatest effect of CR in asphalt binder modification occurs when devulcanization and depolymerization do not take place completely, but the asphalt binder is sufficiently swollen and the reaction is carried out at a partial level of chemical reaction [25].

Moreover, regarding other characteristics of LEA mixtures, Carter et al. examined the compatibility of LEA, HMA, and WMA samples made with Sasobit and Evotherm. In this research, LEA and samples modified with Sasobit were the most compatible samples, followed by HMA and samples made with Evotherm [26]. Olard and Gaudefroy compared the performance and environmental characteristics of LEA and HMA by determining the complex modulus at 15°C and 10 Hz according to European Standard NF EN 12697-26, and it was found that LEA has a lower complex modulus than HMA. This result was presented due to the low mixing and compaction temperatures, as a result of less aging of the asphalt binder and the softness of the mixture. In addition, performing a fatigue test showed lower fatigue resistance of LEA compared to HMA. Another part of this research was the environmental evaluation of the samples. In this evaluation, the published total organic compounds value for LEA was reported to be half of the value recorded for HMA [12]. In another study, Gregory and Harder achieved a significant reduction of pollutants in the LEA production process. According to the results, it was found that LEA production is associated with a 51% reduction in suspended particles, 21% nitrogen oxide, and 82% carbon monoxide. Also, the amount of sulfur oxide and formaldehyde emissions was reported to decrease by 46% and 95%, respectively. Another result of this research was the reduction of fuel consumption so that the energy consumption for the production of LEA showed a 33% reduction compared to HMA [27].

2. Research Objectives

The purpose of this research is to evaluate the rutting and moisture resistance of LEA mixtures. Considering that the effect of additives in LEA modification is the research gap of previous studies, the use of CR to increase the performance characteristics of LEA is considered an innovation of this research. In this regard, the ability of CR to overcome moisture sensitivity and its potential to be replaced with adhesion-enhancing additives is investigated as the first objective of this study by performing the indirect tensile strength test. Also, in order to examine the rutting resistance, the dynamic creep test is used, and by determining FN extracted from four conventional methods, the rutting resistance of asphalt mixtures is compared with each other, and the effect of CR in increasing the rutting resistance of LEA is investigated as the second objective of this research. Moreover, due to the variety of variables in the LEA construction process, the comparison of FN determination models and the introduction of the most stable model are other objectives of this study. In this regard, the trend of FN changes obtained from different models is examined, and finally, the dependence of the models on the mentioned variables is evaluated with statistical analysis.

3. Methodology

3.1. Materials. In this study, limestone aggregate was used to produce LEA mixtures. Table 1 shows the characteristics of used aggregates. The gradation of aggregates, as illustrated in Figure 1, was according to ASTM standards the nominal and maximum sizes of the aggregates are 12.5 mm and 19 mm, respectively. Also, a base asphalt binder with a 60/70 penetration grade prepared from the Jey Oil Refinery was selected. Table 2 shows the physical characteristics of the asphalt binder.

3.2. Additive. According to the studies conducted on CR and the advantages of the wet process in the production of rubberized asphalt mixtures, in this research, this method was used. Also, because of the considerable influence of crumb rubber on the properties of asphalt mixtures in the range of 10–20% by the weight of the binder, CR percentage was limited to this range [28]. Table 3 presents the physical and chemical properties of CR.

On the other hand, research that has been performed regarding the performance of different types of CR shows that CR-modified asphalt binders produced by ambient grinding method with a smaller size have better performance, such as stability, viscosity, stiffness, and moisture and rutting resistance [29]. Therefore, in this research, CR produced by the mentioned method was used with 40 mesh size, and Table 4 represents the gradation of used CR based on ASTM D 5644.

In addition, the asphalt binder temperature during mixing was selected at 180°C, and a high shear mixer with 2000 rpm was used for 2 hours to achieve a homogeneous mixture. Table 5 presents the characteristics of asphalt binders modified with CR in the mentioned percentages.

In this research, two methods of a softening point difference in aluminum tubes and morphology evaluation of the mixture were used to ensure the compatibility of the mixture. In the first method, according to ASTM D7173, modified binders were heated to a temperature of 163°C and poured into aluminum tubes and kept in an oven for

Table 1: Characteristics of limestone aggregates.

Characteristics		Standards	Results		
			Coarse aggregate	Fine aggregate	Filler
Sand equivalent (%)		AASHTO-T176	—	69	—
Los Angeles abrasion loss (%)		AASHTO-T96	17	—	—
Atterberg limits	PI	ASTM-D4318	—	Non-plastic	Non-plastic
	PL		—	—	—
	LL		—	Indeterminate	Indeterminate
Percentage of fractured particles (%)		ASTM-D5821	100	—	—
Boiling water (%)		ASTM-D3625	˂5	—	—
Soundness (5 cycles), sodium sulfate (%)		AASHTO-T104	1	3	—
Water absorption		AASHTO-T84	0.6	1.1	—

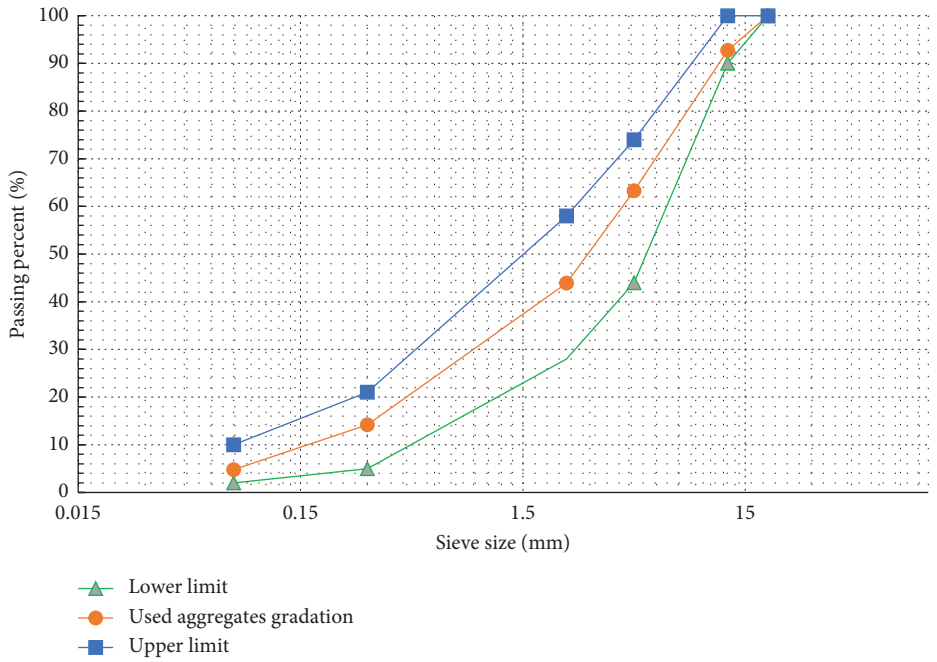

Figure 1: Gradation curve.

Table 2: Characteristics of base asphalt binder.

Characteristics	Standards	Specification values		Results
		Min	Max	
Specific gravity @ 25°C (g/cm^3)	ASTM-D70	—	—	1.016
Penetration @ 25°C (0.1 mm)	ASTM-D6	60	70	63
Softening point (°C)	ASTM-D36	49	56	49.2
Flash point (°C)	ASTM-D92	232	—	305
Kinematic viscosity @ 120°C (cSt)		—	—	773
Kinematic viscosity @ 135°C (cSt)	ASTM-D2170	—	—	342
Kinematic viscosity @ 160°C (cSt)		—	—	141
Heating loss (%)	ASTM-D1754	—	0.8	0.22

48 hours. In the next step, they were placed at a temperature of −18°C for 4 hours. Finally, each sample was cut into three equal parts, and the softening point was determined from their upper and lower parts. As can be seen from Table 6, although the softening point difference is increasing with the increase of CR percentage, the values obtained are lower than 2.5°C. Therefore, it can be assured that the obtained mixtures have good homogeneity and acceptable storage

Table 3: Properties of crumb rubber.

Characteristics		Standards	Specification values		Results
			Min	Max	
Physical	Moisture (%)	ASTM D 1864	—	0.75	0.43
	Density (g/cm^3)	ASTM D 5603-08	—	—	1.15
Chemical	Acetone extractive (%)	ASTM D 297	8	22	19
	Ash (%)		—	8	7.6
	Rubber hydrocarbon (%)		42	—	48

Table 4: Crumb rubber gradation.

Passing percentage (%)	Sieve size (mm)
100	No. 30 (850 μm)
89	No. 40 (600 μm)
57.7	No. 50 (425 μm)
23	No. 80 (300 μm)
18.3	No. 100 (150 μm)

Table 5: Characteristics of crumb rubber-modified binder.

Binder property	Standard	Unit	Crumb rubber percentage			
			0	10	15	20
Softening point	ASTM-D36	˚C	49.2	58.3	61	73.1
Penetration at 25˚C	ASTM-D5	0.1 mm	63	47	43	34
Viscosity at 135˚C	ASTM-D2170	cST	342	717	824	1218
Specific gravity	ASTM-D70	g/cm^3	1.016	1.037	1.041	1.049

Table 6: Storage stability test for modified asphalt binders.

CR percentage	Softening point (˚C)		$S(b)$-$S(t)$
	Top	Bottom	
10	57.8	59.3	1.5
15	60.3	62.2	1.9
20	71.7	74.1	2.4

stability [30]. Another common method to evaluate the compatibility of polymeric asphalt binders is to examine their morphology. For this purpose, preparing scanning electron microscopy (SEM) images is an effective tool, so showing the size, increasing the volume of polymer particles, and how they are distributed inside the asphalt binder are considered advantages of their application. Figure 2 represents an SEM image of the asphalt binder sample modified with 15% CR. As can be seen, CR particles are distributed evenly inside the binder, so CR particles have a homogeneous distribution inside the binder, and no agglomeration is observed in them. In addition, the close distance of CR particles to each other indicates the fact that these particles are sufficiently swollen so that their interparticle distance is decreased. Therefore, it can be expected that CR and asphalt binder have a homogeneous mixture, so they will have good compatibility and storage stability.

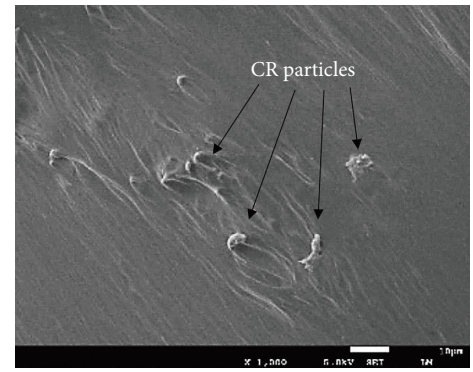

Figure 2: SEM image of the asphalt binder modified with 15% CR.

3.3. Mix Design. In this research, the Superpave volumetric mix design based on the AASHTO R35 standard was used to design the samples. Also, according to the studies conducted on LEA and limiting the maximum size of fine aggregates between 2 and 3 mm, sieve No. 8 was selected for the separation of fine aggregates and coarse aggregates [11, 12, 27].

Considering the necessity of mixing temperature in the range of 80 to 100˚C, the choice of factors, such as the coarse aggregate temperature, asphalt binder temperature, and moisture content of fine aggregates, is decisive in LEA construction. According to NCHRP report 691, the moisture content of fine aggregates is recommended between 3 and 4%. Also, the coarse aggregates should be placed at 170˚C for 4 hours, and fine aggregates should be used at room temperature, and the asphalt binder is utilized at 135˚C [16]. Therefore, in this study, according to NCHRP report 691, firstly, the aggregates were divided into two categories, fine and coarse, by sieve No. 8. Then, enough water was added to the fine fraction, which included 44% of the weight of aggregates, and the final moisture content reached 3.5%. Simultaneously, coarse aggregates and asphalt binder were heated to 170 and 135˚C, respectively. Afterward, the coarse aggregates were mixed with the asphalt binder in a wire mixer. After ensuring the complete coating of the obtained mixture, fine aggregates were added to the mixture. Sudden contact of moisture with the hot mixture caused the formation of foam according to Figure 3. At this stage, the mixing of the mixture was continued until fine aggregates were completely coated. After the mixing operation, the desired samples were compacted according to the AASHTO T312 standard, and their characteristics were determined, as

Figure 3: Foam in LEA.

indicated in Table 7, in which G_{mm} is the maximum theoretical specific gravity, G_{mb} is the bulk specific gravity, V_a is the air voids, VMA is the voids in mineral aggregates, VFA is the voids filled with asphalt, and OBC is the optimum binder content.

3.4. Experimental Program

3.4.1. Moisture Sensitivity Test. The most common method for the evaluation of moisture sensitivity is the modified Lottman test, which is performed according to AASHTO T283. In this regard, six compacted cylindrical samples are made with air voids of 6–8%. Then, the samples are divided into two categories. The first category is considered unconditioned or control samples, and the second one, as conditioned samples, after obtaining 70–80% saturation and being placed at −18°C for 16 hours, is kept in a water bath at 60°C temperature for 24 hours. Finally, by performing the indirect tensile strength (ITS) test with a loading rate of 50 mm/min at a temperature of 25°C and recording ITS values, the tensile strength ratio (TSR) is determined through equation (1), where ITS_{wet} and ITS_{dry} (kPa) are the indirect tensile strength for the conditioned and dry samples, respectively [31].

$$\text{Tensile strength ratio (TSR)} = \frac{ITS_{wet}}{ITS_{dry}}. \tag{1}$$

3.4.2. Dynamic Creep Test. In this research, the uniaxial dynamic creep test was performed according to NCHRP report 465 by applying a repetitive shear haversine loading by a universal testing machine (UTM). First, the test samples were made in 7% air void and a cylindrical mold according to AASHTO T312, and after coring, samples with a diameter of 100 mm and a height of 150 mm were extracted. Since permanent deformation occurs at high temperatures, in this research, the test temperature was selected as 54.4°C according to the recommendation of the aforementioned report. The samples were then transferred to the loading frame, and LVDTs were installed on it to record the deformations created during the test. First, a constant load equal to 5% of the final load was applied. Then, haversine loading was introduced to the samples with a period of 0.1 seconds of loading and 0.9 seconds of rest time, and the loading continued until the failure of the samples or reaching 10000 cycles. In this research, according to the recommendation of the aforementioned report, the uniaxial dynamic creep test was performed at the stress level of 207 kPa. Also, in order to evaluate the rutting susceptibility of LEA to the increase in stress level, all samples were also tested at the stress level of 310 kPa. Then, ascending diagrams consisting of accumulated strain against loading cycles were drawn for each of the samples. These diagrams, which consist of three different areas, are known as creep curves. In the first area, as the loading cycle increases, the strain increases at a decreasing rate. In the second area, the strain increases at a constant rate, and finally, in the third area, the strain increases at an increasing rate. The number of cycles related to the starting point of this area is known as flow number (FN), and it is used to evaluate the rutting resistance of asphalt mixtures [32]. Many models have been presented to determine the location of FN, the definition of four of which has been discussed in the following.

(1) Three-Stage Model. This model was presented to interpret the creep diagram by Zhou et al. According to the proposed model, the power law model according to equation (2) was used to interpret the first area of creep curves. Also, a simple linear model according to equation (3) was used to interpret the second area. On the other hand, due to the rapid increase in the permanent strain after the second area, a model according to equation (4) was presented to describe the third area [33].

$$\text{Primary stage: } \varepsilon_P = aN^b.\ N < N_{ps}, \tag{2}$$

$$\begin{aligned}\text{Secondary stage: } \varepsilon_P &= \varepsilon_{PS} + c\left(N - N_{PS}\right).\ \varepsilon_{PS} \\ &= aN_{PS}^b, N_{PS} \le N \le N_{ST},\end{aligned} \tag{3}$$

$$\begin{aligned}\text{Tertiary stage: } \varepsilon_P &= \varepsilon_{ST} + \mathrm{d}\left(e^{f\left(N - N_{ST}\right)} - 1\right).\ \varepsilon_{ST} \\ &= \varepsilon_{PS} + c\left(N_{ST} - N_{PS}\right), N \ge N_{ST,}\end{aligned} \tag{4}$$

in which a, b, c, d, and f are materials constants, ε_{ST} is the accumulated plastic strain at the tertiary stage beginning, ε_{PS} is the accumulated plastic strain at the secondary area beginning, N_{ST} is the number of cycles at the tertiary stage beginning, N_{PS} is the number of cycles at the secondary stage beginning, ε_P is plastic strain, and N is the number of cycles.

(2) FNest Method. This method was presented by Archilla et al. [34]. First, the strain rate is measured using equation (5), where N is the cycle number, ε_{PNi+1} is the permanent strain at the $N+1$ cycle and ε_{PNi-1} is the permanent strain at the $N-1$ cycle.

$$\frac{\partial\left(\varepsilon_P\right)i}{\partial N} = \frac{\left(\varepsilon_{PNi+1} - \varepsilon_{PNi-1}\right)}{2\Delta N}. \tag{5}$$

Then, the five-point moving average period technique is performed to smooth the strain rate values obtained from

Table 7: Volumetric properties of asphalt mixtures.

Sample	CR (%)	G_{mm}	G_{mb}	V_a (%)	VMA (%)	VFA (%)	OBC (%)	Mixing temperature (°C)	Compaction temperature (°C)
HMA	0	2.449	2.353	3.920	14.971	73.816	4.6	160	135
LEA	0	2.466	2.368	3.968	14.244	72.145	4.4	90	90
LEA10	10	2.447	2.351	4.010	15.057	73.368	4.6	92	90
LEA15	15	2.449	2.353	3.934	15.162	74.054	4.8	92	90
LEA20	20	2.451	2.354	3.939	15.453	74.051	5.2	98	90

equation (5). Also, the range of load cycles applied is defined by equation (6), where FN_{MAP5} is the minimum point of this strain rate, N_{lb} is the lower number of cycles, N_{ub} is the highest number of cycles, C is 0.5, and N_{max} is the maximum cycle number.

$$\begin{aligned}[N_{lb}, N_{un}] = [\,&\max(100, FN_{MAP5} - C \times FN_{MAP5}),\\ &\min(N_{max}, FN_{map5} + C \times FN_{MAP5}.\end{aligned} \tag{6}$$

In this method, it is assumed that $N_{UB} \leq N_{max}$. Hence, when $N_{UB} > N_{max}$, N_{UB} is considered equal to N_{max}. By using the obtained data and the above explanations, equation (7) is used for fitting the data, where α, β, and γ denote probability distribution parameters.

$$\varepsilon_P = \frac{1}{\beta}\left[-\ln\left(1 - \frac{N}{\gamma}\right)\right]\frac{1}{\alpha}. \tag{7}$$

It is worth mentioning that these parameters are obtained from the solver tool in Excel. By determining the above parameters, FN is obtained.

(3) Francken Model. Billgiri et al. used a combined mathematical model for determining FN [35], which is derived from the Francken model and is defined as equation (8), where A, B, C, and D are regression coefficients, N is the loading cycle, and ε_p (N) is the permanent strain.

$$\varepsilon_P(N) = AN^B + C\left(e^{DN} - 1\right). \tag{8}$$

These parameters are determined by using a statistical package and regression technique. Then, the strain slope is obtained by the following equation:

$$\frac{d\varepsilon_P}{dN} = \left(A \times B \times N^{(B-1)}\right) + \left(C \times D \times e^{D \times N}\right). \tag{9}$$

Finally, FN is obtained with the second differentiation of ε_p (N). In this case, FN is at the point that the values obtained from equation (10) change their sign from negative to positive.

$$\frac{d^2\varepsilon_P}{dN^2} = A \times B \times (B-1) \times N^{(B-2)} + \left(C \times D^2 \times e^{D \times N}\right). \tag{10}$$

(4) Stepwise Method. Goh and You presented a simple and step-by-step method to identify the beginning of the third area by modifying the traditional method [36]. According to the mentioned method, in the first step, the permanent strain obtained from the test is smoothed by the reallocating technique. This operation is performed by assuming that the permanent strain either remains constant or increases during the loading cycles. In the second step, the strain rate is measured according to equation (11), and eventually, FN is obtained by identifying the location of the min amount of strain rate.

$$\text{Strain Rate} = \frac{\varepsilon}{N}, \tag{11}$$

where N is the loading cycle, and ε is the permanent strain.

4. Results and Discussion

4.1. Moisture Sensitivity. As can be seen from ITS values represented in Table 8, the LEA sample has a lower ITS value than the HMA sample in both dry and conditioned states. The reason for this is the presence of many pores due to the confinement of part of the water vapor created in the process of making LEA in the asphalt binder and, as a result, easier penetration of water to the surface of aggregates [37]. The modification of asphalt binder by CR increases the viscosity of the asphalt binder, so it results in a thicker coating of asphalt binder on aggregates and its greater adhesion, and consequently, an increase in the resistance of the mixture and its integrity. Therefore, with the addition of CR up to 15% of binder weight, this asphalt mixture experiences a significant increase in ITS value, so that the ITS value recorded for the LEA15 sample in dry and conditioned conditions was 1.52 and 1.77 times this parameter, respectively, compared to LEA sample. With the increase in the percentage of CR from 15 to 20%, due to the excessive increase in asphalt binder viscosity, and consequently, the decrease in the efficiency of the mixture, the LEA20 sample experienced a decrease in coverability, adhesion, and cohesion, and therefore, ITS value for it in both dry and wet conditions was significantly reduced compared to LEA15 sample.

Another part of the information presented in Table 8 is related to TSR values recorded for control and LEA samples. In this evaluation, as expected, the LEA sample with a TSR value of 0.62 showed high moisture sensitivity. The low moisture resistance of this sample is due to the low viscosity of the asphalt binder, low quality of aggregate coating, and as a result, easier penetration of water due to the presence of many pores left in the bituminous coating because of the creation of water vapor during mixing [38]. By adding CR to LEA samples, the moisture resistance increased significantly, so that the application of 10% additive resulted in a 27% increase in TSR value in the LEA10 sample compared to the LEA sample without additive. With the increase in the percentage of CR, a downward trend was observed in the

Table 8: Results of the moisture sensitivity test.

Sample	ITS_{dry} (kPa)	ITS_{wet} (kPa)	TSR
HMA	932	764	0.82
LEA	552	342	0.62
LEA10	737	582	0.79
LEA15	841	606	0.72
LEA20	779	491	0.63

TSR values of LEA samples, so that LEA15 and LEA20 samples with a TSR of 0.72 and 0.63, respectively, faced a 10% and 25% decrease in the value of this parameter compared to LEA10 sample. The decrease in moisture resistance in the mentioned samples was due to the excessive stiffness of the asphalt binder and its inability to properly cover the aggregates and more opportunity for moisture to penetrate their surface. The studies performed on the performance of CR-modified samples against moisture damage indicate that these types of asphalt mixtures, despite their high resistance to rutting, have low moisture resistance, and only a small content of CR can lead to a decrease in moisture sensitivity [15, 39–41]. The point to consider in this evaluation is the inability of CR to compensate for the drop in the moisture resistance of LEA samples compared to HMA samples [39]. As can be seen from the results, although LEA10 and LEA15 samples met the lowest recommended value for this test, the highest TSR recorded in this evaluation was assigned to the HMA sample. Therefore, CR, despite its proven benefits, seems not to be a suitable alternative to antistripping additives for LEA, especially in areas with high rainfall and situations with a high probability of moisture damage. Therefore, antistripping additives should be applied in the production of CR-modified LEA mixtures in the mentioned situations.

4.2. Creep Curves. Figures 4(a) and 4(b) present the permanent strain diagrams according to the loading cycle obtained from the dynamic creep test at the stress level of 207 and 310 kPa, respectively. It is evident that LEA15 and LEA20 samples have a better performance against rutting by recording lower accumulated strain during loading cycles. LEA and LEA20 samples showed the weakest performance, respectively, and the HMA sample is placed between the two mentioned groups. By adding CR to the asphalt binder, the rubber polymer chains absorb the aromatic part of the asphalt binder, which creates a gel-like state in the asphalt binder and increases its elasticity and viscosity. These interactions strengthen the internal network of asphalt binder and cause its thicker coating on aggregates, increasing cohesion and, ultimately, higher rutting resistance of mixtures. As can be seen from the diagrams, by increasing the CR percentage, the LEA20 sample represented a drop in resistance to rutting. This is considered due to the excessive absorption of asphalt binder's light oils by rubber particles and, as a result, excessive increase of its viscosity, the results of which were also observed in previous studies with increasing CR from 15 to 20% [23, 42]. Hence, as the viscosity increases, the workability of the mixture is reduced during the mixing time, and consequently, this results in a weaker coverage of aggregates and low cohesion and integrity of the mixture. Another noteworthy point in this evaluation is the low resistance of LEA samples against permanent deformation compared to other samples. The excessive weakness of this sample due to the low mixing temperature compared to the HMA sample is the lower viscosity and aging of the asphalt binder, which has led to the softening of the mixture and the reduction of stiffness.

4.3. Flow Number. Figures 5(a) and 5(b) represent FN values obtained from the three-stage, FNest, Francken, and stepwise models at two levels of stress 207 and 310 kPa, respectively. It is obvious from the results that, apart from the stepwise model, other methods were successful in determining FN in all test samples, and the mentioned method was only able to determine FN in the HMA sample, LEA20 sample at 207 kPa level of stress, and LEA, LEA10, and LEA15 samples at 310 kPa level of stress. According to the results obtained from the four mentioned models, the LEA sample has the lowest FN value in both stress levels as expected. The low rutting resistance of the LEA sample is due to the less aging of the asphalt binder and, as a result, its excessive softness [16]. By using CR in LEA samples and its physicochemical reaction with the asphalt binder, the viscosity of the asphalt binder is increased, and as a result, the coating on the aggregates is improved. This has caused an increase in the adhesion between the aggregates and has finally led to an increase in the rutting resistance of LEA samples. Also, with the start of the chemical reaction of the asphalt binder and CR, new cross-linking bonds have been formed between the asphalt binder and CR, which has created a three-dimensional reinforcing network in the structure of the mixture. Therefore, the use of CR in the asphalt binder leads to an increase in the integrity and elasticity of the mixture, so that by using 10% CR, the LEA10 sample has a significant increase in FN and has a higher FN value than the LEA sample and even HMA sample. By increasing the amount of CR to 15%, the LEA sample still experienced an upward trend in FN, the result of which can be clearly observed in the study of other researchers [23, 43]. In this research, the modification of asphalt binder to the mentioned amount has resulted in an increase in FN value by 2 times for the LEA15 sample compared to the HMA sample in all the mentioned models. By increasing the amount of CR to 20%, the LEA sample faced a significant decrease in the amount of FN, similar to previous research [44]. The drop in rutting resistance of the LEA20 sample is due to the high viscosity of asphalt binder, the low mixing temperature of the LEA production process, and the low ability of asphalt binder in coating aggregates, which has resulted in a decrease in FN value compared to HMA sample.

On the other hand, comparing FN results obtained from the mentioned methods shows that the stepwise model provides the highest FN value in all test samples. Also, in the situation where FN obtained from the three-stage model has higher values, FNest and Francken models provided the

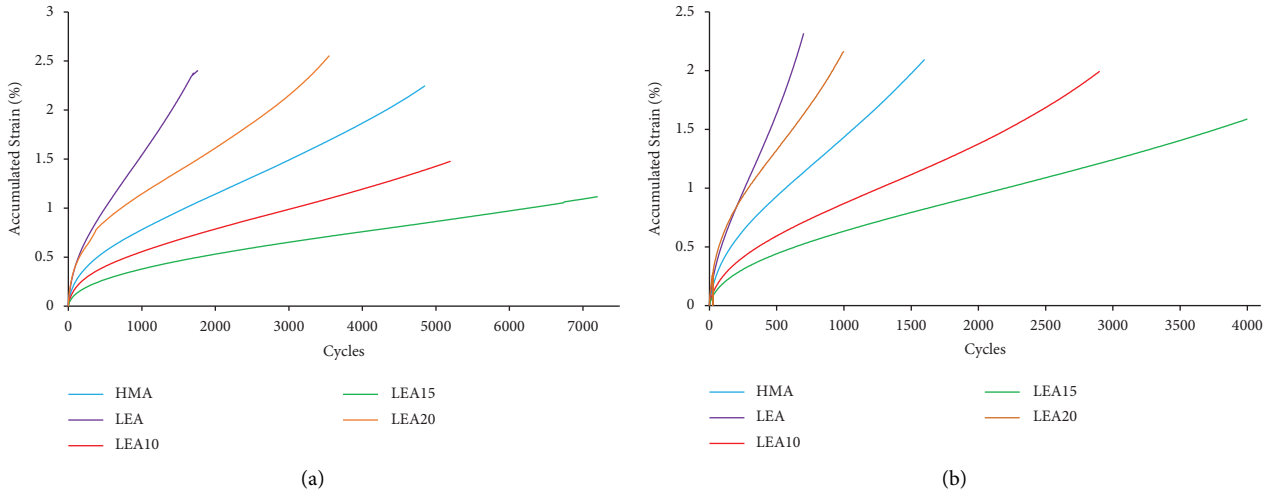

Figure 4: Creep curves of test samples at the stress level of (a) 207 kPa and (b) 310 kPa.

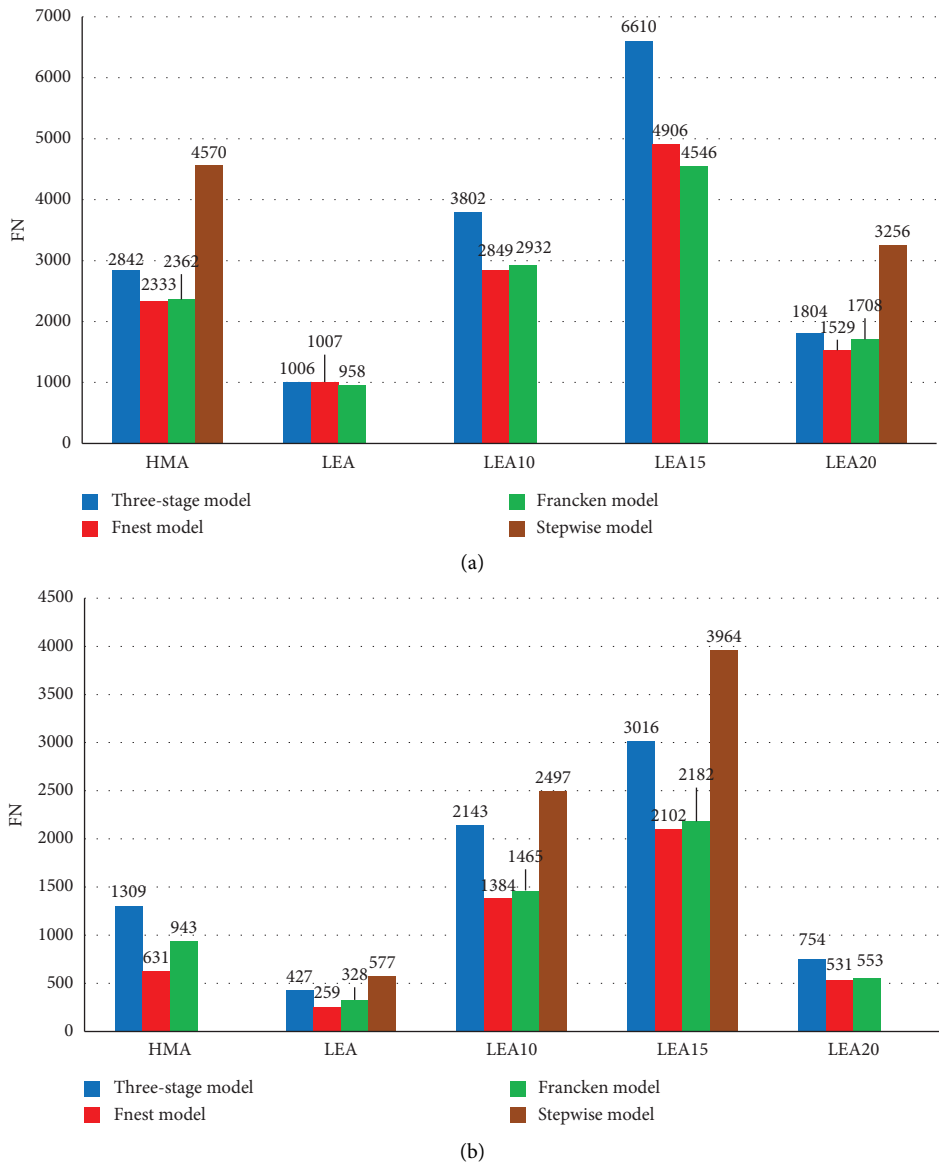

Figure 5: FN values obtained from the models at (a) 207 kPa and (b) 310 kPa.

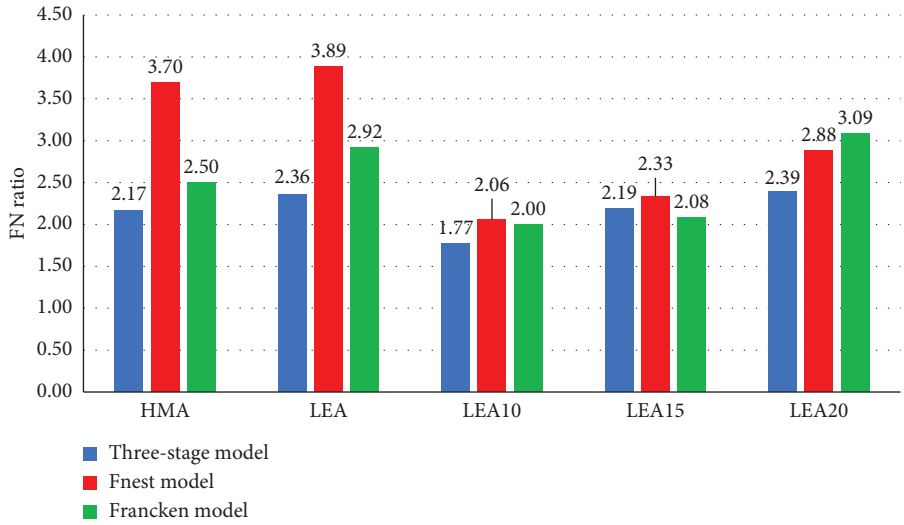

Figure 6: Changes in FN with respect to the increase in the stress level.

lowest value of this index with relatively similar FNs compared to other methods.

Figure 6 shows the changes in FN with respect to the increase in the stress level. It is necessary to mention that due to the inability of the stepwise model to provide FN for all samples, it was not possible to calculate FN changes for it. As can be seen from the results, with the increase in the stress level from 207 to 310 kPa, FN ratio changes have presented a different trend, which is also true in the other three models. Although LEA15 provides the highest FN and is the most resistant sample against rutting, LEA10 has the lowest FN ratio. Therefore, this sample has the lowest decrease in FN with the increase in the stress level and provides the lowest sensitivity to the increase in the stress level. By increasing the amount of CR to 15%, the effect of the additive can still be observed in reducing the sensitivity to the stress level increase, so that LEA15 has a lower value of this ratio than the remaining three samples. The important point in this evaluation is the almost identical process of the three-stage and Francken models in presenting the order of the results of the rutting susceptibility. Also, determining the amount of correlation between different models according to Figure 7 shows that the three-stage and Francken models have the highest correlation coefficient (R^2) value, so it can be concluded that these models have more correlation to each other. But the important point about the FN ratio extracted from the three-stage and Francken models is that the LEA20 sample, despite having higher FN values than the LEA sample, has shown more sensitivity to the stress level. This can be due to the negative effect of increasing the additive percentage and, as a result, the excessive absorption of the binder oil part by the rubber particles and the brittleness of this sample in the face of high stress levels.

Figures 8–12 show the location of FN in the creep curves obtained from the test samples. As can be seen from the results, in LEA, LEA10, and LEA15 samples at the stress level of 207 kPa and HMA and LEA20 samples at the stress level of 310 kPa, even though the creep curves have entered the third area after passing through the second area, the stepwise model was not able to determine FN. In addition, in HMA and LEA20 samples at 207 kPa level of stress and LEA10, LEA, and LEA15 samples at the stress level of 310 kPa, FN obtained by the mentioned method is located in the third area, and its location is contradictory to the definition of FN based on the junction of the second and third areas. Therefore, it seems that the stepwise model is not a reliable method to determine FN in this research. Also, by observing the location of FN obtained from other methods, this fact can be achieved although it seems that FN obtained from the three-stage model is closer to the third area in all test samples, and the results of the other two methods are generally located on the straight line; however, the judgment in this regard is difficult, and choosing the best model requires more investigation. Therefore, in the next section, statistical analysis has been conducted to determine the best model and compare FN values extracted from the mentioned models.

4.4. Statistical Analysis

4.4.1. Investigating the Methods of Determining FN. For determining the appropriateness and correlation of results obtained from various models, the ANOVA test was used according to Tables 9 and 10 in two levels of stress 207 and 310 kPa, respectively, and the mean difference of FN obtained from different models was compared.

According to the comparison, the lowest mean difference in both stress levels was assigned to Fnest and Francken models. Therefore, the mentioned models showed the highest correlation in FN values, the result that was also observed in the research conducted by Ameri et al. by achieving similar FN values compared to other models [45]. Another noteworthy point in this comparison is the high correlation between the results of the

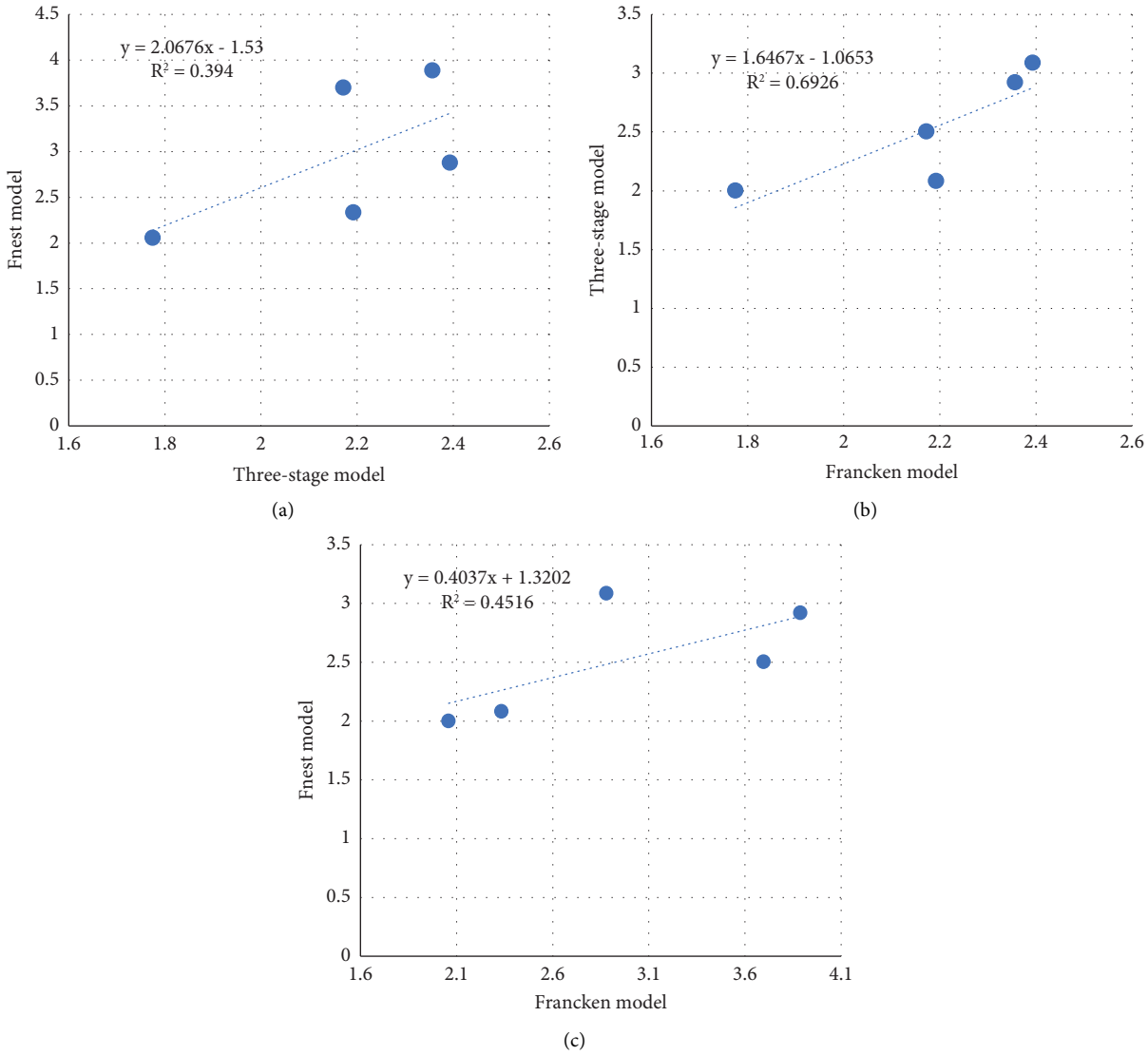

Figure 7: Correlation between FN ratio obtained from (a) three-stage and Fnest models, (b) Francken and three-stage models, and (c) Francken and Fnest models.

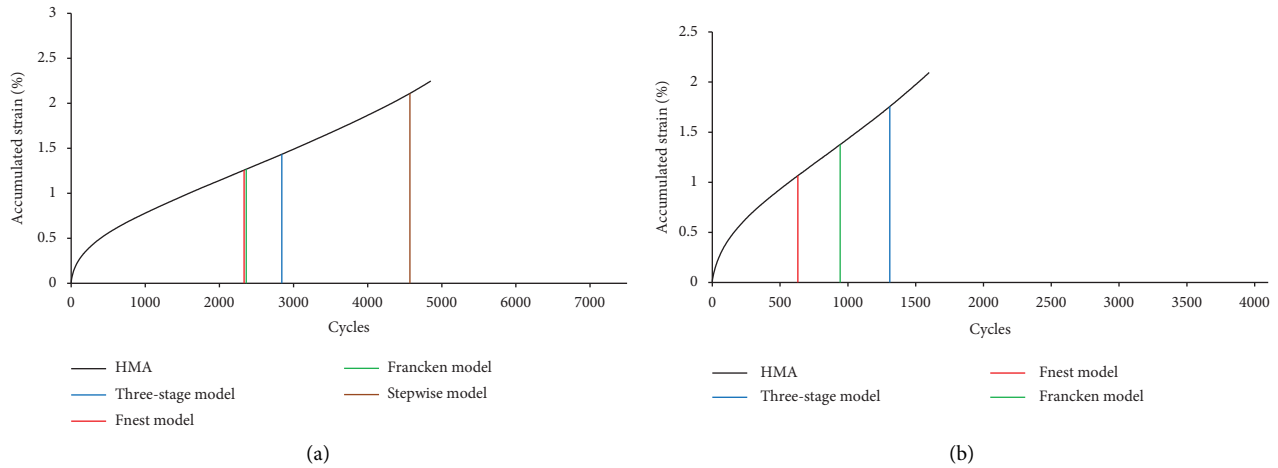

Figure 8: Location of FN values obtained from the models for HMA sample at the stress level of (a) 207 kPa and (b) 310 kPa.

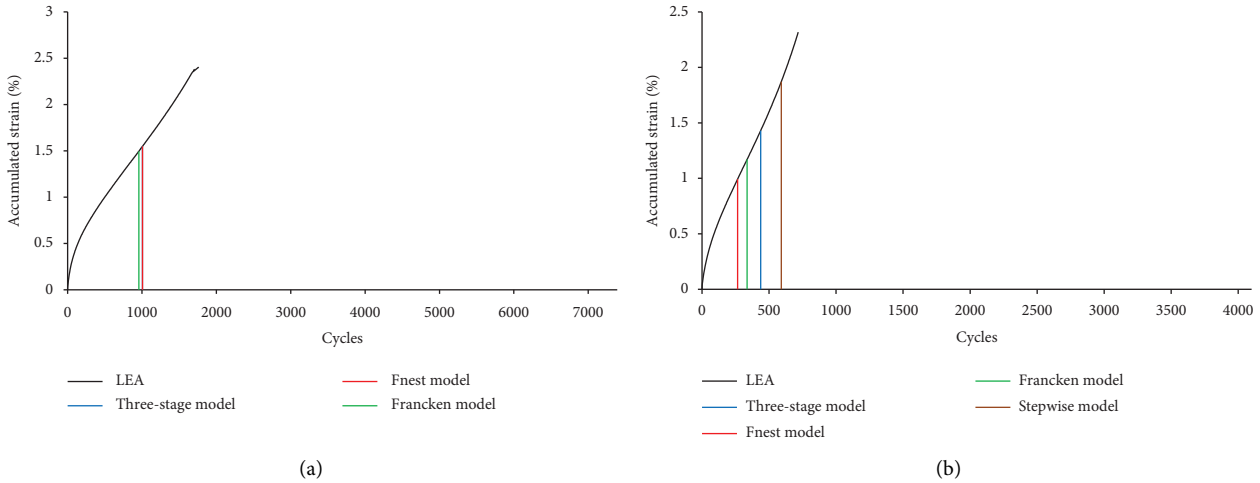

Figure 9: Location of FN values obtained from the models for LEA sample at the stress level of (a) 207 kPa and (b) 310 kPa.

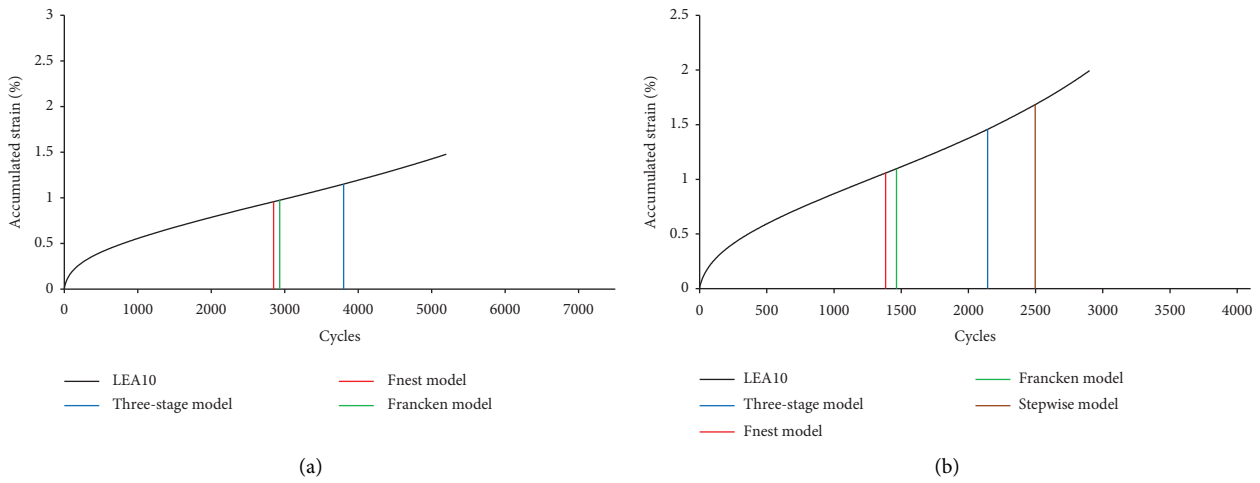

Figure 10: Location of FN values obtained from the models for LEA10 sample at the stress level of (a) 207 kPa and (b) 310 kPa.

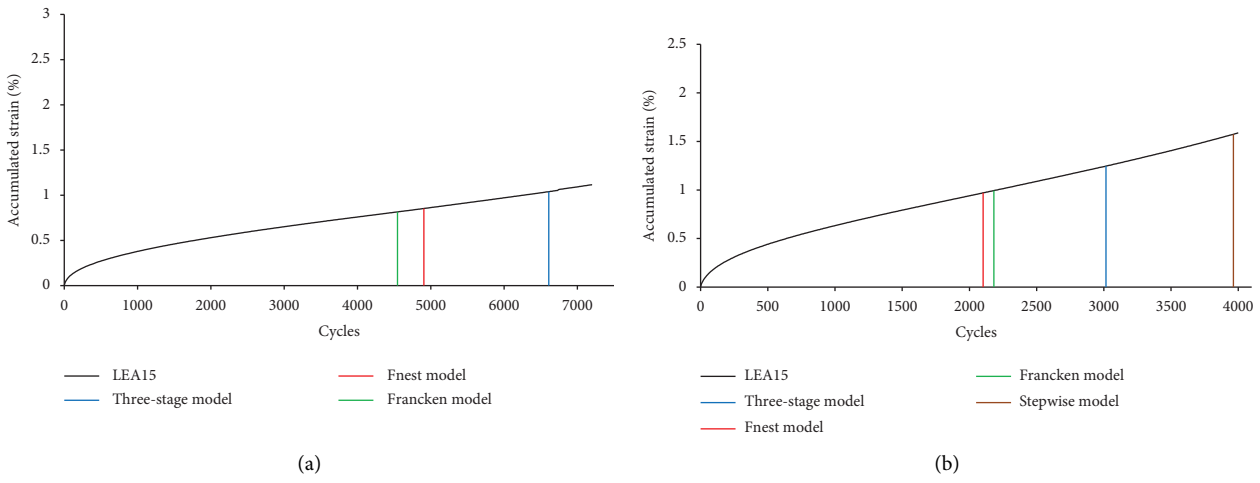

Figure 11: Location of FN values obtained from the models for LEA15 sample at the stress level of (a) 207 kPa and (b) 310 kPa.

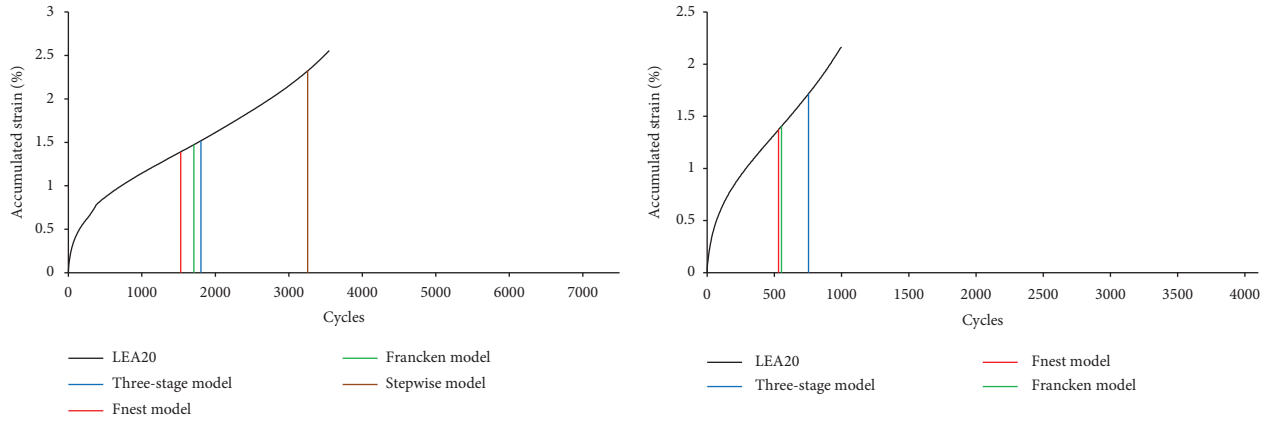

Figure 12: Location of FN values obtained from the models for LEA20 sample at the stress level of (a) 207 kPa and (b) 310 kPa.

Table 9: Multiple comparisons for all models at the stress level of 207 kPa.

(I) group	(J) group	Std. error	Mean difference (I-J)	Sig.	95% Confidence interval	
					Lower	Upper
Three-stage model	Fnest model	1056.08485	688.00000	0.526	−1593.5326	2969.5326
	Francken model	1056.08485	711.60000	0.512	−1569.9326	2993.1326
	Stepwise model	1397.06894	−700.20000	0.625	−3718.3839	2317.9839
Fnest model	Three-stage model	1056.08485	−688.00000	0.526	−2969.5326	1593.5326
	Francken model	1056.08485	23.60000	0.983	−2257.9326	2305.1326
	Stepwise model	1397.06894	−1388.20000	0.339	−4406.3839	1629.9839
Francken model	Three-stage model	1056.08485	−711.60000	0.512	−2993.1326	1569.9326
	Fnest model	1056.08485	−23.60000	0.983	−2305.1326	2257.9326
	Stepwise model	1397.06894	−1411.80000	0.331	−4429.9839	1606.3839
Stepwise model	Three-stage model	1397.06894	700.20000	0.625	−2317.9839	3718.3839
	Fnest model	1397.06894	1388.20000	0.339	−1629.9839	4406.3839
	Francken model	1397.06894	1411.80000	0.331	−1606.3839	4429.9839

Table 10: Multiple comparisons for all models at the stress level of 310 kPa.

(I) group	(J) group	Std. error	Mean difference (I-J)	Sig.	95% Confidence interval	
					Lower	Upper
Three-stage model	Fnest model	648.30841	548.40000	0.412	−842.0832	1938.8832
	Francken model	648.30841	435.60000	0.513	−954.8832	1826.0832
	Stepwise model	748.60207	−816.20000	0.294	−2421.7918	789.3918
Fnest model	Three-stage model	648.30841	−548.40000	0.412	−1938.8832	842.0832
	Francken model	648.30841	−112.80000	0.864	−1503.2832	1277.6832
	Stepwise model	748.60207	−1364.60000	0.090	−2970.1918	240.9918
Francken model	Three-stage model	648.30841	−435.60000	0.513	−1826.0832	954.8832
	Fnest model	648.30841	112.80000	0.864	−1277.6832	1503.2832
	Stepwise model	748.60207	−1251.80000	0.117	−2857.3918	353.7918
Stepwise model	Three-stage model	748.60207	816.20000	0.294	−789.3918	2421.7918
	Fnest model	748.60207	1364.60000	0.090	−240.9918	2970.1918
	Francken model	748.60207	1251.80000	0.117	−353.7918	2857.3918

stepwise model and the three-stage model. According to the obtained results, the mentioned models provide the lowest mean difference, and therefore, they have the best fit compared to others. Studies conducted by other researchers such as Goh et al. also represent the high correlation of the mentioned models by calculating R^2 value [36, 46].

4.4.2. Between-Sample Variability. A between-sample variability is an approach that is used to account for the variability of results for similar replicates. This solution is used when only one method is used to calculate the results [45]. Table 11 and Figure 13 present the coefficient of variation (CV) of FN for asphalt samples in each of the three methods of three-stage, FNest, and

Table 11: Results of between-sample variability.

Sample	Three-stage model		Fnest model		Francken model	
	207 (kPa)	310 (kPa)	207 (kPa)	310 (kPa)	207 (kPa)	310 (kPa)
HMA	2842	1309	2333	631	2362	943
LEA	1006	427	1007	259	958	328
LEA10	3802	2143	2849	1384	2932	1465
LEA15	6610	3016	4906	2102	4546	2182
LEA20	1804	754	1529	531	1708	553
STD	2173	1055	1509	753	1360	746
AVE	3213	1530	2525	981	2501	1094
CV (%)	68	69	60	77	54	68

Note. CV was obtained by dividing the standard deviation (STD) by the average (AVE).

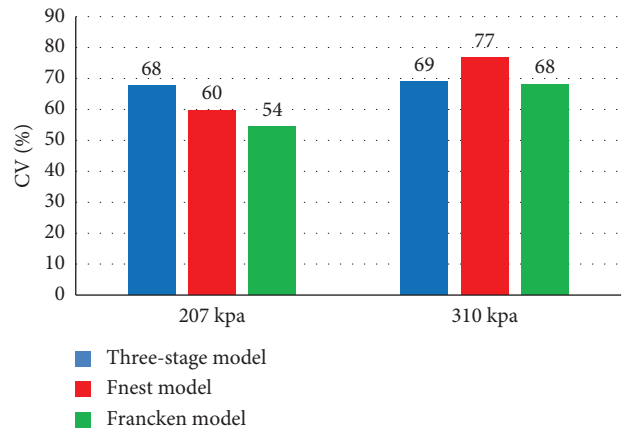

Figure 13: Between-sample variability.

Francken. It should be mentioned that in this analysis, the stepwise model is removed due to the inability to determine FN for most of the samples and providing insufficient data. In this research, due to the existence of many variables in the construction of asphalt mixture samples, such as mixing and compaction temperatures, humidity, additive percentage, air voids, and asphalt binder percentage, as well as changes in the stress level, between-sample variability can be a suitable method to determine a model with the lowest sensitivity to the mentioned variables [45]. As can be seen from the results, at the stress level of 207 kPa, the three-stage model provides the highest CV in determining FN. Therefore, the mentioned method does not have enough stability and has the most changes in the results. At this stress level, the Francken model shows fewer changes than other models; therefore, the mentioned model has less dependence on the variety of asphalt samples and the changes in stress levels, and it can be considered the most stable model compared to others. Also, at the stress level of 310 kPa, the highest CV belongs to the Fnest model. At this stress level, although the three-stage model shows less dependence on the variables, the Francken model still has the lowest CV, the result of which was also obtained in the research conducted by Ameri et al. [45]. Therefore, as it is suggested in AASHTO T378, the use of the Francken model is recommended to determine the FN of LEA mixtures since it is less sensitive to variables.

5. Conclusion

In this research, by modifying LEA with CR in three weight percentages of 10, 15, and 20, evaluating the moisture and rutting resistance of LEA samples was conducted. Also, the comparison of FN determination models and the introduction of the most stable model were performed. According to the obtained results, it was found that:

(i) In the moisture resistance results, although LEA10 and LEA15 samples met the minimum requirement in the ITS test, the TSR value recorded for these samples was still lower than that for the HMA sample. Therefore, it is recommended to utilize antistripping additives when using LEA-containing CR, especially in areas with a high probability of moisture damage.

(ii) Investigating creep curves obtained from the dynamic creep test at 54.4°C and two stress levels of 207 and 310 kPa showed that LEA without additive had the highest amount of accumulated strain during the loading cycle compared to other samples. Also, by adding CR, a significant decrease in the accumulated strain of LEA samples was observed, so that the creep curves recorded for LEA10 and LEA15 samples were in a much better condition than HMA. By increasing the amount of CR to 20%, the accumulated strain experienced a significant increase.

(iii) FN values obtained by different methods at two levels of 207 and 310 kPa showed that LEA15 and LEA10 samples had the highest FN value, respectively. In this evaluation, HMA was in a better condition than LEA20, and LEA was recognized as the weakest sample with the lowest FN value.

(iv) The evaluation of the rutting susceptibility of laboratory samples to an increase in the stress level showed that LEA10 and LEA20 samples, respectively, provide the lowest FN changes with respect to the stress level increase. On the other hand, considering the variety of variables in the construction process of LEA compared to HMA, the comparison of FN determination models showed that the Francken model had less dependence on the variety of LEA samples and stress levels than other

models, and it is recommended as the most stable model to determine FN for LEA samples.

(v) For future studies, various nanomaterials and fibers can be applied in this regard [47, 48]. In addition, other failures of LEA mixtures containing CR and nanomaterials can be investigated [49, 50]. The use of electric vehicles and clean fuels can also help reduce the carbon footprint in the pavement industry [51–53]. In addition, other statistical analyses can be incorporated with the proposed approaches [54–56]. Various modeling methods and algorithms are recommended for further investigation in the continuation of this research [57–59]. Different validation methods are recommended in this regard [60, 61]. Optimization algorithms can also be used to obtain the optimal additive content [62–64]. Moreover, deep learning techniques can be applied to present more accurate results [65, 66]. Other types of asphalt binders with different penetration grades are also recommended to be used in a study to compare their results.

Data Availability

The data used to support the findings of this study are available from the corresponding author upon request.

Disclosure

In this study, Iranian governmental organizations have not been partners and sponsors, and this study is purely studious.

Conflicts of Interest

The authors declare that they have no conflicts of interest.

References

[1] A. F. Hashmi, M. S. Khan, M. Bilal, M. Shariq, and A. Baqi, "Green concrete: an eco-friendly alternative to the OPC concrete," *Construction*, vol. 2, no. 2, pp. 93–103, 2022.

[2] F. Faghihinejad, M. Mohammadi Fard, A. Roshanghalb, and P. Beigi, "A framework to assess the correlation between transportation infrastructure access and economics: evidence from Iran," *Mathematical Problems in Engineering*, vol. 2022, pp. 1–15, 2022.

[3] A. Shayesteh, E. Ghasemisalehabadi, M. W. Khordehbinan, and T. Rostami, "Finite element method in statistical analysis of flexible pavement," *Journal of Marine Science and Technology*, vol. 25, no. 2, p. 15, 2017.

[4] N. C. Ming, R. P. Jaya, H. Awang, N. L. S. Ing, M. R. M. Hasan, and Z. H. Al-Saffar, "Performance of glass powder as bitumen modifier in hot mix asphalt," *Physics and Chemistry of the Earth*, Parts A/B/C, vol. 128, Article ID 103263, 2022.

[5] M. Khordehbinan and M. R. Kaymanesh, "Chemical analysis and middle-low temperature functional of waste polybutadiene rubber polymer modified bitumen," *Petroleum Science and Technology*, vol. 38, no. 1, pp. 8–17, 2020.

[6] M. Zarei, A. A. Kordani, A. Naseri, M. W. Khordehbinan, M. khajehzadeh, and M. Zahedi, "Evaluation of fracture behaviour of modified warm mix asphalt containing vertical and angular cracks under freeze-thaw damage," *International Journal of Pavement Engineering*, pp. 1–17, 2022.

[7] F. Autelitano, E. Garilli, and F. Giuliani, "Half-warm mix asphalt with emulsion. An experimental study on workability and mechanical performances," *Transportation Research Procedia*, vol. 55, pp. 1081–1089, 2021.

[8] P. Caputo, A. A. Abe, V. Loise et al., "The role of additives in warm mix asphalt technology: an insight into their mechanisms of improving an emerging technology," *Nanomaterials*, vol. 10, no. 6, p. 1202, 2020.

[9] B. Kheradmand, R. Muniandy, L. T. Hua, R. B. Yunus, and A. Solouki, "An overview of the emerging warm mix asphalt technology," *International Journal of Pavement Engineering*, vol. 15, no. 1, pp. 79–94, 2014.

[10] A. J. Kadhim, M. Y. Fattah, and N. M. Asmael, "Evaluation of the moisture damage of warm asphalt mixtures," *Innovative Infrastructure Solutions*, vol. 5, no. 2, p. 54, 2020.

[11] H. Zelelew, C. Paugh, M. Corrigan, S. Belagutti, and J. Ramakrishnareddy, "Laboratory evaluation of the mechanical properties of plant-produced warm-mix asphalt mixtures," *Road Materials and Pavement Design*, vol. 14, no. 1, pp. 49–70, 2013.

[12] F. Olard and V. Gaudefroy, "Laboratory Assessment of Mechanical Performance and Fume Emissions of LEA® HWMA (90 C) vs. Traditional HMA (160 C)," in *Proceedings of the 2nd International warm-mix conference*, France, October 2012.

[13] S. C. Some, V. Gaudefroy, and D. Delaunay, "Warm mix asphalt: mechanical performance assessment and coating quality evaluation," in *Proceedings of the 2nd International Symposium on Asphalt Pavement and Environment*, TRANSPORTATION RESEARCH BOARD, USA, June 2012.

[14] M. M. Hilal and M. Y. Fattah, "Evaluation of resilient modulus and rutting for warm asphalt mixtures: a local study in Iraq," *Applied Sciences*, vol. 12, no. 24, Article ID 12841, 2022.

[15] H. Ziari, H. Divandari, S. M. Seyed Ali Akbar, and S. M. Hosseinian, "Investigation of the effect of crumb rubber powder and warm additives on moisture resistance of SMA mixtures," *Advances in Civil Engineering*, vol. 2021, pp. 1–12, 2021.

[16] R. F. Bonaquist, *Mix design practices for warm mix asphalt*, Transportation Research Board, USA, 2011.

[17] M. Samadi and N. Jahan, "Determining the effective level of outrigger in preventing collapse of tall buildings by IDA with an alternative damage measure," *Engineering Structures*, vol. 191, pp. 104–116, 2019.

[18] M. Samadi and N. Jahan, "Comparative study on the effect of outrigger on seismic response of tall buildings with braced and RC wall core. I: optimum level and examining modal response spectrum analysis reliability," *The Structural Design of Tall and Special Buildings*, vol. 30, no. 8, p. e1848, 2021.

[19] H. Seraji, R. Tavakkoli-Moghaddam, and R. Soltani, "A two-stage mathematical model for evacuation planning and relief logistics in a response phase," *Journal of Industrial and Systems Engineering*, vol. 12, no. 1, pp. 129–146, 2019.

[20] M. Kazemidemneh and M. Mahdavinejad, "Use of space syntax technique to improve the quality of lighting and modify energy consumption patterns in urban spaces," *European Journal of Sustainable Development*, vol. 7, no. 2, p. 29, 2018.

[21] M. Rajabi, M. Habibpour, S. Bakhtiari, F. M. Rad, and S. Aghakhani, "The development of BPR models in smart cities using loop detectors and license plate recognition

technologies: a case study," *Journal of Future Sustainability*, vol. 3, no. 2, pp. 75–84, 2023.

[22] S. Saeedi, "Investigation of the construction supply chain vulnerabilities under an unfavorable macro-environmental context," in *Proceedings of the 30th Annual Conference of the International Group for Lean Construction*, IGLC30, Edmonton, Canada, June 2022.

[23] A. Ameli, R. Babagoli, S. Asadi, and N. Norouzi, "Investigation of the performance properties of asphalt binders and mixtures modified by Crumb Rubber and Gilsonite," *Construction and Building Materials*, vol. 279, Article ID 122424, 2021.

[24] D. Lo Presti, G. Airey, and P. Partal, "Manufacturing terminal and field bitumen-tyre rubber blends: the importance of processing conditions," *Procedia-Social and Behavioral Sciences*, vol. 53, pp. 485–494, 2012.

[25] I. Mohammadi and H. Khabbaz, "Challenges associated with optimisation of blending, mixing and compaction temperature for asphalt mixture modified with crumb rubber modifier (CRM)," in *Applied Mechanics and Materials*, vol. 256, 2013

[26] A. Carter, O. Mainardis, and D. Perraton, "Design of Half-Warm Asphalt Mixes with Additives," 2010, https://trid.trb.org/view/910146.

[27] A. Gregory and P. E. Harder, "LEA Halfwarm Mix Paving Report," 2007, http://www.lea-uk.biz.

[28] S. Bressi, N. Fiorentini, J. Huang, and M. Losa, "Crumb rubber modifier in road asphalt pavements: state of the art and statistics," *Coatings*, vol. 9, no. 6, p. 384, 2019.

[29] D. Jones, Y. Liang, and J. Harvey, *Performance Based Specifications: Literature Review on Increasing Crumb Rubber Usage by Adding Small Amounts of Crumb Rubber Modifier in Hot Mix Asphalt*, University of California Pavement Research Center, California, USA, 2017.

[30] W. Zheng, H. Wang, Y. Chen, J. Ji, Z. You, and Y. Zhang, "A review on compatibility between crumb rubber and asphalt binder," *Construction and Building Materials*, vol. 297, Article ID 123820, 2021.

[31] H. Ziari, B. Mojaradi, S. A. Saadatjoo, A. Amini, V. Najafi Moghaddam Gilani, and S. M. Hosseinian, "Laboratory investigation of reclaimed asphalt mixtures containing cyclogen and vacuum bottom rejuvenators," *Advances in Civil Engineering*, vol. 2023, Article ID 6223569, 11 pages, 2023.

[32] M. Q. Ismael, H. H. Joni, and M. Y. Fattah, "Neural network modeling of rutting performance for sustainable asphalt mixtures modified by industrial waste alumina," *Ain Shams Engineering Journal*, vol. 14, no. 5, Article ID 101972, 2023.

[33] F. Zhou, T. Scullion, and L. Sun, "Verification and modeling of three-stage permanent deformation behavior of asphalt mixes," *Journal of Transportation Engineering*, vol. 130, no. 4, pp. 486–494, 2004.

[34] A. R. Archilla, L. G. Diaz, and S. H. Carpenter, "Proposed method to determine the flow number in bituminous mixtures from repeated axial load tests," *Journal of Transportation Engineering*, vol. 133, no. 11, pp. 610–617, 2007.

[35] K. P. Biligiri, K. E. Kaloush, M. S. Mamlouk, and M. W. Witczak, "Rational modeling of tertiary flow for asphalt mixtures," *Transportation Research Record*, vol. 2001, no. 1, pp. 63–72, 2007.

[36] S. W. Goh and Z. You, "A simple stepwise method to determine and evaluate the initiation of tertiary flow for asphalt mixtures under dynamic creep test," *Construction and Building Materials*, vol. 23, no. 11, pp. 3398–3405, 2009.

[37] G. Shiva Kumar and S. Suresha, "State of the art review on mix design and mechanical properties of warm mix asphalt," *Road Materials and Pavement Design*, vol. 20, no. 7, pp. 1501–1524, 2019.

[38] X. Wang, Z. Fan, L. Li, H. Wang, and M. Huang, "Durability evaluation study for crumb rubber–asphalt pavement," *Applied Sciences*, vol. 9, no. 16, p. 3434, 2019.

[39] H. H. Joni and A. H. Abed, "Evaluation the moisture sensitivity of asphalt mixtures modified with waste tire rubber," in *Proceedings of the IOP Conference Series: Earth and Environmental Science*, IOP Publishing, Baghdad, Iraq, 2022.

[40] A. Ameli, N. Norouzi, E. H. Khabbaz, and R. Babagoli, "Influence of anti stripping agents on performance of binders and asphalt mixtures containing Crumb Rubber and Styrene-Butadiene-Rubber," *Construction and Building Materials*, vol. 261, Article ID 119880, 2020.

[41] A. Cetin, "Effects of crumb rubber size and concentration on performance of porous asphalt mixtures," *International Journal of Polymer Science*, vol. 2013, Article ID 789612, 10 pages, 2013.

[42] B. Bairgi, Z. Hossain, and R. D. Hendrix, "Investigation of rheological properties of asphalt rubber toward sustainable use of scrap tires," *IFCEE*, pp. 359–368, 2015.

[43] M. Ameri, N. Nezafat, S. Eskandari, M. Shahsavari, and A. A. Yousefi, "The potential of intrinsically disordered regions in vaccine development," *Expert Review of Vaccines*, vol. 21, pp. 1–3, 2022.

[44] S. Liu, W. Cao, J. Fang, and S. Shang, "Variance analysis and performance evaluation of different crumb rubber modified (CRM) asphalt," *Construction and Building Materials*, vol. 23, no. 7, pp. 2701–2708, 2009.

[45] M. Ameri, A. H. Sheikhmotevali, and A. Fasihpour, "Evaluation and comparison of flow number calculation methods," *Road Materials and Pavement Design*, vol. 15, no. 1, pp. 182–206, 2014.

[46] N. Barazi Jomoor, M. Fakhri, and M. R. Keymanesh, "Determining the optimum amount of recycled asphalt pavement (RAP) in warm stone matrix asphalt using dynamic creep test," *Construction and Building Materials*, vol. 228, Article ID 116736, 2019.

[47] S. Rezaei, M. Khordehbinan, S. M. R. Fakhrefatemi, S. Ghanbari, and M. Ghanbari, "The effect of nano-SiO2 and the styrene butadiene styrene polymer on the high-temperature performance of hot mix asphalt," *Petroleum Science and Technology*, vol. 35, no. 6, pp. 553–560, 2017.

[48] S. M. Hosseinian, V. Najafi Moghaddam Gilani, P. Mehraban Joobani, and M. Arabani, "Investigation of moisture sensitivity and conductivity properties of inductive asphalt mixtures containing steel wool fiber," *Advances in Civil Engineering*, vol. 2020, Article ID 8890814, 9 pages, 2020.

[49] G. H. Hamedi, M. R. Esmaeeli, V. Najafi Moghaddam Gilani, and S. M. Hosseinian, "The effect of aggregate-forming minerals on thermodynamic parameters using surface free energy concept and its relationship with the moisture susceptibility of asphalt mixtures," *Advances in Civil Engineering*, vol. 2021, Article ID 8818681, 15 pages, 2021.

[50] S. Rezaei, Seyed Mohsen Damadi, Ali Edrisi, Mansour Fakhri, and Mohammad Worya Khordehbinan, "Fatigue analysis of bitumen modified with composite of nano-SiO2 and styrene butadiene styrene polymer," *Frattura Ed Integrità Strutturale*, vol. 14, no. 53, pp. 202–209, 2020.

[51] A. Kazemtarghi, "Active Compensation-Based Harmonic Reduction Technique to Mitigate Power Quality Impacts of EV Charging Systems," *IEEE Transactions on Transportation Electrification*, vol. 9, no. 1, 2022.

[52] A. Razmjoo, A. Ghazanfari, M. Jahangiri et al., "A comprehensive study on the expansion of electric vehicles in europe," *Applied Sciences*, vol. 12, no. 22, Article ID 11656, 2022.

[53] A. Kazemtarghi, A. Mallik, and Y. Chen, "Dynamic Pricing Strategy for Electric Vehicle Charging Stations to Distribute the Congestion and Maximize the Revenue," *Applied Energy*, vol. 326, 2023.

[54] H. Bozorgkhou and M. Alimohammadirokni, "Studying and investigating the impact of marketing mix factors on e-purchase via smart phones (case study: digikala corporation)," *Nexo Revista Científica*, vol. 35, no. 04, pp. 992–1003, 2022.

[55] F. Faghihinejad and S. Monajem, "Pathology of the disabled people access to public transport and prioritizing practical solution," *Tobacco Regulatory Science (TRS)*, pp. 7634–7643, 2021.

[56] G. Shen, "Fault analysis of machine tools based on grey relational analysis and main factor analysis," in *Journal of Physics: Conference Series*, vol 1069, IOP Publishing, 2018.

[57] E. Eslami and H. B. Yun, "Improvement of multiclass classification of pavement objects using intensity and range images," *Journal of Advanced Transportation*, vol. 2022, Article ID 4684669, 20 pages, 2022.

[58] M. Mehrara, M. A. Majdzadeh, and A. Ghazanfari, "Determinants of private investment in Iran based on bayesian model of averaging," *The Journal of Economic Policy*, vol. 7, no. 14, pp. 1–29, 2016.

[59] Y. Zhang, L. Mu, G. Shen, Y. Yu, and C. Han, "Fault diagnosis strategy of CNC machine tools based on cascading failure," *Journal of Intelligent Manufacturing*, vol. 30, no. 5, pp. 2193–2202, 2019.

[60] S. Haghir, R. Haghnazar, S. Saghafi Moghaddam, D. Keramat, M. R. Matini, and K. Taghizade, "BIM based decision-support tool for automating design to fabrication process of freeform lattice space structure," *International Journal of Space Structures*, vol. 36, no. 3, pp. 164–179, 2021.

[61] R. M. Rastegar, S. Saghafi Moghaddam, R. Haghnazar, and C. Zimring, "From evidence to assessment: developing a scenario-based computational design algorithm to support informed decision-making in primary care clinic design workflow," *International Journal of Architectural Computing*, vol. 20, no. 3, pp. 567–586, 2022.

[62] H. Seraji, R. Tavakkoli-Moghaddam, S. Asian, and H. Kaur, "An location-allocation model for humanitarian logistics with distributive injustice and dissatisfaction under uncertainty," *Annals of Operations Research*, vol. 319, no. 1, pp. 211–257, 2022.

[63] G. Shen, W. Zeng, Y. Zhang, C. Han, and P. Liu, "Determination of the average maintenance time of CNC machine tools based on type II failure correlation," *Eksploatacja i Niezawodnosc Maintenance and Reliability*, vol. 19, no. 4, pp. 604–614, 2017.

[64] M. Sadeghi, M. Nikfar, and F. Rad, "Optimizing warehouse operations for environmental sustainability: a simulation study for reducing carbon emissions and maximizing space utilization," *Journal of Future Sustainability*, vol. 4, no. 1, pp. 35–44, 2024.

[65] E. Eslami and H.-B. Yun, "Attention-based multi-scale convolutional neural network (A+ MCNN) for multi-class classification in road images," *Sensors*, vol. 21, no. 15, p. 5137, 2021.

[66] C. Han and X. Fu, "Challenge and opportunity: deep learning-based stock price prediction by using Bi-directional LSTM model," *Frontiers in Business, Economics and Management*, vol. 8, no. 2, pp. 51–54, 2023.